Title: Aerogel insulation materials for industrial installation : properties and structure of new factory-made products

Author: Artur Miros, Bronisław Psiuk, Barbara Szpikowska-Sroka

Citation style: Miros Artur, Psiuk Bronisław, Szpikowska-Sroka Barbara. (2017). Aerogel insulation materials for industrial installation : properties and structure of new factory-made products. "Journal of Sol-Gel Science and Technology" (2017, iss. 3, s. 496-506), doi 10.1007/s10971-017-4539-0

UNIWERSYTET ŚLĄSKI
W KATOWICACH

Biblioteka
Uniwersytetu Śląskiego

Ministerstwo Nauki
i Szkolnictwa Wyższego

CrossMark

INVITED PAPER: SOL-GEL AND HYBRID MATERIALS FOR ENERGY, ENVIRONMENT AND BUILDING APPLICATIONS

Aerogel insulation materials for industrial installation: properties and structure of new factory-made products

Artur Miros[1] · Bronisław Psiuk[2] · Barbara Szpikowska-Sroka[3]

Abstract In this article the comparisons of two new factory-made Chinese aerogel products with the Pyrogel® product, all available on the market, are presented. The aerogel products are in a flexible blanket form and all products are dedicated for high temperature applications. The properties of the samples such as their dimension stability, water vapour transmission and water absorption are also described. Additionally the microstructure and chemical composition of the products are analysed using SEM/EDS (scanning electron microscopy coupled with X-ray energy-dispersive spectroscopy). The differences in the maximum service temperature are presented. The internal self-heating of the aerogel samples is described and is compared to a similar effect observed in mineral wool samples. The results in the change of the thermal properties in a wide range of temperatures (+ 10–600°C) are shown. The obtained results are correlated with the mineral wool data. The correlation shows an advantage in a high-efficiency thermal performance of aerogel products compared to other insulation materials at high temperatures.

Graphical Abstract
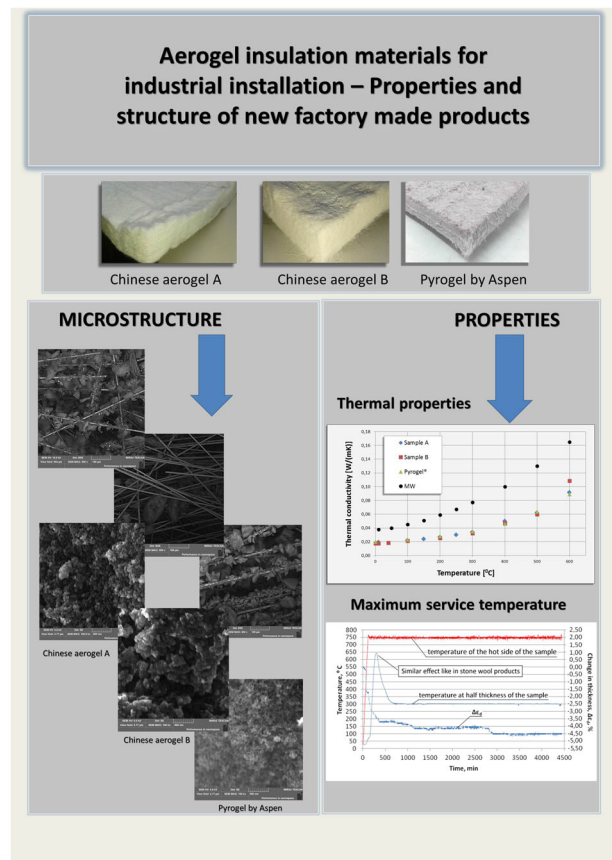
✉ Artur Miros
a.miros@imbigs.pl

1   Institute of Mechanised Construction and Rock Mining, Branch in Katowice, Centre of Low-Energy Buildings Technology and Environmental Management, al. Korfantego 193A, 40-157 Katowice, Poland

2   Refractory Materials Division in Gliwice, Institute of Ceramics and Building Materials, ul. Toszecka 99, 44-100 Gliwice, Poland

3   Institute of Chemistry, University of Silesia, ul. Szkolna 9, 40-007 Katowice, Poland

1 Introduction

Among the most important parameters of thermal insulation materials are their thermal properties, and in addition their safety in case of fire. On the market, there are a large group of products characterized by low thermal conductivity (below 0.04 W/m·K), and good thermal parameters. For building applications, the main products are: expanded polystyrene (EPS) [1] and mineral wool [2, 3], which exist next to other products such as polyurethane/poly-isocyanurate (PUR/PIR) [4, 5], phenolic foams [6, 7] or thermal insulation composites such as vacuum insulation panels [8–10]. The application of aerogel products is not very common due to the limited commercial products currently available, and the costs of such applications in comparison to the most popular thermal insulation materials [11–13].

For high temperature industrial installations, in the case of maximum service temperature of the thermal insulation materials, some of the products cannot be applied due to the risk of thermal (and/or other) property lost. The organic insulation materials have low maximum service temperatures compared to the inorganic ones. The highest resistance on temperature treatment of PIR products can reach a 200°C service temperature. Other products are characterized by lower service temperatures such as 175 °C for flexible elastomeric foam, 120 °C for phenolic foam and up to 100°C for EPS and extruded polystyrene [14].

Generally, for high temperature installations, inorganic materials such as mineral or ceramic wool and aerogel products are most popular. For example, the maximum service temperature of glass and stone wool (called mineral wool) is around 500 and 800 °C, respectively, and for ceramic wool, it is around 1700 °C.

For high temperature installations, the cost of insulation materials is not as important as for building applications, especially that the payback period can be much shorter, due to energy heat loss [15]. So, more expensive products such as aerogel blankets are more often used due to their much better thermal properties than mineral or ceramic wool. The better thermal properties of aerogel products imply wider applications. Lower thermal conductivity of the material allows for the opportunity to use thinner layers and less volume of insulation material. Moreover, the whole application process is faster and lower amount of material is needed. Very often in an existing high temperature installation one can find places where it is impossible to maintain the necessary level of thermal insulation, e.g. in places where two pipe systems intersect in close proximity to each other or where pipes run along a wall or other closely located units of installation. In such cases, to obtain a satisfactory result in thermal modernization and the reduction of energy heat loss, a thin product, with high thermal properties is useful, and provides more options for designing new industrial insulations. The factory-made aerogel products on the market dedicated to industrial applications generally come from two producers [16, 17]. The aim of this paper was to investigate the suitability of two Chinese factory-made aerogel products for high temperature industrial applications now available on the market and compare them with well-known Aspen product (http://host.web-print-design.com/aerogel/history.htm. Accessed 10 April 2017) called Pyrogel® [16]. The thermal properties on a whole range of temperatures were performed using the steady-state heat transfer method of guarded hot plate apparatus (GHP) apparatus. The maximum service temperature was determined by a self-made heating box in accordance with a specific standard. Sensitivity to atmospheric conditions (water/vapour) was tested based on properties such as dimension stability, water vapour transmission and water absorption. The structure and chemical composition were tested using scanning electron microscopy coupled with X-ray EDS.

2 Materials and sample

Two types of factory-made Chinese aerogel blankets currently available on the market have been investigated (Fig. 1). One of them, hereafter referred to as Product A, is DRT06 from Guangdong Alison Hi-Tech Co., Ltd. The second one, hereafter referred to as Product B, is FMD 650 from Nano Tech Co., Ltd. The intended use of these products, declared by the manufacturers, are applications for industrial installations (high temperatures). Comparison with Pyrogel® aerogel blankets from Aspen Aerogels Inc.

| Product A | Product B | Pyrogel® |

Fig. 1 The Products A, B and Pyrogel® aerogel blankets

Table 1 Specifications of the aerogel blanket Products A, B and Pyrogel®: thicknesses, densities and maximum service temperatures of the products as declared by their producers

Properties	Product A	Product B	Pyrogel®
Thickness (mm)	10	10	10
Density (kg/m^3)	195	185	200
Maximum service temperature (°C)	750	650	650

Table 2 Highest and lowest values thickness, density and colour for A, B and Pyrogel® samples

Properties	Sample A	Sample B	Pyrogel®
Thickness (mm)	11–15	10–15	10–13
Density (kg/m^3)	175–185	155–170	195–210
Colour	White	White	Beige

dedicated to industrial, high temperature applications was performed.

Product A has a declared thickness of 10 mm and a density of 195 kg/m^3, while Product B has a declared thickness of 10 mm and a density of 185 kg/m^3. The maximum service temperatures declared by the manufacturers are 750 and 650 °C, respectively. The specifications of the products are shown in Table 1. The Pyrogel® product is available with two different thicknesses: 5 and 10 mm. For this study, the 10 mm Pyrogel® product was chosen. The maximum service temperature declared by the producer is 650 °C with a density of 200 kg/m^3 [16]. The specifications of the Pyrogel® product are also shown in Table 1.

The range of thicknesses and densities for each product sample investigated in this paper were determined and presented in Table 2.

3 Methodology

3.1 Sample preparation

The samples were cut to a general size of 300×300 mm^2 from the middle of a blanket in order to avoid the damages and defects which may occur at the edges. The samples were conditioned at room temperature (23 ± 2) °C and at a relative humidity (RH) of $50 \pm 5\%$. Only steady-state weight samples were used for testing. Dimensional parameters (thickness, length, width) and the mass of the samples were recorded before every test treatment.

3.2 Thickness, length, width and density

The length and width measurements were carried out in accordance with EN 822:2013 [18] by measuring the

dimension on a flat surface using a caliper (accuracy ± 0.01 mm).

The thickness of each investigated samples (Table 2) was determined according to EN 823:2013 [19]. The measured sample was placed on a stiff reference surface, and a pressure plate was put on the top of the sample. To determine the distance between the reference surface and the pressure plate, the dial gauge (accuracy ± 0.01 mm) was mounted on a rigid frame attached to a flat base plate. The dimension of the square pressure plate was 300×300 mm^2. The pressure on the sample was 50 kPa. To determine the range of thicknesses, 10 samples of dimensions 300×300mm^2 were measured. Each individual result was recorded and the average value was calculated.

In order to perform the dimensional stability (3.4), the thickness was measured using a caliper (accuracy ± 0.01 mm) at five places on the sample (one in the middle and four at each half length of the sample side). Each individual result was recorded and the average value was calculated.

The density was determined using a balance with ± 0.1 g accuracy. The density was calculated based on 10 individual samples (300×300 mm^2) with known thickness, length and width. Each individual result of the investigated A, B and Pyrogel® samples was recorded.

3.3 Scanning electron microscope characterization

The microscopic measurements were done on a Scanning Electron Microscope (SEM) Mira III from Tescan, equipped with a Aztek Automated X-ray microanalysis system (based on an X-ray energy-dispersive spectroscopy (EDS) method) from Oxford Instruments. The investigations were performed in both low vacuum and high vacuum modes. The low vacuum mode allowed for the observation of the as-received samples. For the second mode the samples required some additional preparation; namely, a small amount of the sample was fixed on a carbon tape and purged in order to remove the loose components and then the carbon was evaporated. The high vacuum mode in contrast to the low vacuum mode allowed for the observation of the aerogel's topography at high magnifications and gare a more precise estimate of the specimen's chemical composition using the EDS method.

3.4 Dimensional stability

Dimensional stability under specified temperature and humidity condition was carried out in accordance with EN 1604:2013 [20]: 23 °C with an RH of 90% and 70 °C with an RH of 90%. In each case, the storage time was 48 h. The sample size was 200×200 mm^2.

To obtain 23 °C with an RH of 90% condition, the samples were placed into a conditioning chamber (with the

same function as a desiccator). It was a glass box with a size of 700×700 mm^2 and a height of 500 mm. The cover of the chamber was sealed by a gasket. Inside the chamber there was a metallic screen where the samples were placed. The metallic screen was positioned on small polystyrene blocks (10 cm high) to allow free circulation of air in the whole chamber. Under the metallic screen (on the bottom of the chamber, between the small polystyrene blocks) a beaker with saturated KNO_3 solution was placed to provide 90% humidity in the chamber. To ensure that the humidity was uniform in the conditioning chamber, a fan was placed over the sample, which operated throughout the conditioning time. Humidity was controlled by LB-705 (LAB-EL) thermohygrometer (uncertainty: temperature ± 0.1 °C, humidity ± 2.0%). To obtain 70 °C and an RH of 90%, the samples were placed into the Brabender Realtest climatic chamber and set to the required parameters.

Length, width, thickness and mass of the samples were registered before and after tests. The mean value of the dimensional stabilities were obtained from three individual results.

3.5 Water vapour transmission

Water vapour transmission was performed according to EN 12086:2013 [21] to determine the flow rate of the water vapour across the samples between two environments with different RH ("dry" state and "humid" state). Water vapour transmission was measured under isothermal conditions. The "dry state" environment was obtained by a calcium chloride desiccant. To achieve the "humid state" environment, saturated aqueous potassium nitrate solution was used. Due to the differences in the partial water vapour pressure in the "dry" state and the "humid" state environments, water vapour flowed through the sample. The rate of water vapour flowing across the sample under a steady-state condition was determined by periodic weighing. The calculation of the water vapour diffusion resistance factor μ was based on the time change of the test, saturated aqueous potassium nitrate solution mass, the exposed area of the sample, the thickness of the sample and the water vapour pressure difference between the two environments. The mean value was obtained from five test results.

3.6 Water absorption

Water absorption was performed by total immersion in water according to EN 12087:2013 [22]. The sample was completely immersed in water over a period of 28 days, but every 7 days the test specimen was turned over. The initial dimensions of the sample was 300×300 mm^2, and the temperature of the water bath was 23 ± 1 °C. The value of the water absorption was calculated as the difference of the

mass sample after 28 days of immersion and the initial mass. The mean value was obtained from five test results.

3.7 Maximum service temperature

The determination of the maximum service temperature— the highest temperature at which the insulation product continues to function within the specified limits of performance—was conducted according to EN 14706:2012 [23]. The initial dimensions of the sample was 300×300 mm^2 and the thickness was at least 100 mm below the 500 Pa load. Due to the required thickness of 100 mm, each sample consisted a multilayer system (10 layers with each dimension of 300×300 mm^2 ca. 10 mm). Generally, the thicknesses of insulation materials for industrial installations (e.g. mineral wool, polyethylene foam, flexible elastomeric foam) are tested according to the above tests.

The samples were heated on one side at a rate of 5°C/min up to the estimated/expected maximum service temperature. This value was maintained for 72 h within a ± 10°C deviation. The temperature on the hot side and at half of the thickness of the sample was continuously measured during heat treatment. The thickness of the sample was recorded during these measurements. The maximum service temperature was determined by calculating the dimensional changes of thickness, $\Delta\varepsilon_d$, in percentage with a maximum assumed not to exceed 5%.

3.8 Thermal conductivity test

Thermal conductivity in the whole range of temperatures was measured on a two-plate guarded hot plate apparatus, GHP 456 Titan from Netzsch, according to EN 12667:2001 [24], which measures steady-state heat transfer through a flat sample. This method gives the absolute thermal conductivity measurement without any required calibration and reference material. Two samples are placed between the plates: a hot plate with a guarded heater and an auxiliary heater (the cold plate). During the measurement a given temperature difference (ΔT) was set between the hot and cold plates over the sample thickness. When the steady-state heat transfer (thermal equilibrium) was reached the hot plate power was measured.

Because of the two-plate apparatus, two samples were needed for testing thermal conductivity; they were selected with a 2% difference thickness range. The thickness was adjusted using specially prepared calcium silicate spacers. Due to increasing uncertainty of the test for thickness samples below 15 mm, tests were performed using two samples placed one over the other. The mean thickness of the samples taken from the upper and lower samples were as follows: for sample A—22.2 mm, for sample B—22.1 mm and for the Pyrogel® sample—21.5 mm. The samples

were conditioned up to constant weight at $23 \pm 2\ °C$ and at a RH of $50 \pm 5\%$. The samples were measured at a atmospheric pressure in the mean temperature range between 10 and 300 °C, and between 300 and 600 °C in a nitrogen atmosphere due to the safety of the GHP apparatus. The temperature difference (ΔT) was set up as follows: at a mean temperature of 10 °C—ΔT was 20 K, in the range of mean temperatures from 100 to 300 °C—ΔT was 60 K and in the range of mean temperatures from 400 to 600 °C—ΔT was 100 K.

For each temperature of the test, the estimated time for the steady-state condition of heat flow was around 24 h.

4 Results

4.1 Dimensional stability, water vapour transmission and water absorption

The results of dimensional stability, water vapour transmission and water absorption by total immersion of sample A, sample B and the Pyrogel® aerogel blankets are presented in Table 3. Differences of dimensional stability between the two different temperatures (23 and 70 °C) were observed for each sample, but were rather small.

Differences between samples appeared in the μ values of water vapour transmission. This parameter describes how many times a tested material is less vapour permeable compared to the same thickness of the air layer (e.g. the μ value for mineral wool is 1, the μ value for EPS is from ca. 30 to 250, the μ value for vapour barriers start from ca. 10,000). The water vapour transmission for sample A is higher than that for sample B and it can be correlated with the higher density of sample A than that of sample B. However, the water vapour transmission is also very sensitive to the defects and fractures inside the sample. The main reason for the variation in the water absorption by

immersion results probably from the quality of the hydrophobization of the tested samples.

The values of water vapour transmission and water absorption by immersion for all the investigated samples are at a level which allow for the avoidance of corrosivity of the metal parts of an installation.

4.2 SEM characterization

The SEM measurement images show transversal cuts of the aerogel specimen. Micrographs presented in Figs. 2 and 3 were collected at various magnifications and various vacuum modes. In Fig. 2 the micrographs have been obtained in low vacuum modes adequate for the observation of the as-received samples. In Fig. 3 the micrographs have been obtained in high vacuum modes adequate for the observation of the aerogels' topography at high magnifications, and to estimate the samples' chemical composition.

Observation of the aerogels in the as-received state (Fig. 2) revealed that they were filled with fibrous material. It seems, in the case of sample A and the Pyrogel samples, that the adhesion of aerogel particles to fibres is stronger than that in sample B. Thus, in sample B the proportion of aerogels per fibre looks the smallest. It should be emphasized that this observation can be not representative for the volume of the sample. The aerogel granules could simply disconnect from the fibres while preparing the test specimen (removing the sample piece from the larger piece of material). Undoubtedly, the difference between the samples concerns the thickness of the fibres. In sample A they are clearly thicker than in the other samples. More accurate measurements of the fibre diameters obtained from the micrographs provided the following results: the diameter of fibres was 9–12 μm for sample A, 6–10 μm for sample B and 5–10 μm for the Pyrogel® sample. It can be added that fibres are a typical addition to aerogels to improve the strength of the product (strength and toughness) [25, 26].

Table 3 Results of dimensional stability, water vapour transmission and water absorption by immersion of sample A, sample B and Pyrogel® aerogel blankets

	Dimensional stability (%)						Water vapour transmission (μ)	Water absorption by immersion (kg/m³)
	Length, $\Delta\varepsilon_l$		Width, $\Delta\varepsilon_w$		Thickness, $\Delta\varepsilon_t$			
	23 °C	70 °C	23 °C	70 °C	23 °C	70 °C		
Sample A	0.0	0.1	0.0	0.1	0.0	0.2	4.8	0.7
Sample B	0.0	0.3	0.1	0.2	0.1	0.5	3.0	1.3
Pyrogel®	0.0	0.2	0.1	0.2	0.0	0.3	4.9	0.5

The dimensional stability was performed at two different temperatures (23 and 70 °C) in a relative humidity of 90%. The uncertainty of thickness measurement is 0.15%, and the length and width is 0.05% at a confidence level of 95%. The uncertainty of the water vapour transmission is 3% and the water absorption by immersion is 2% at a confidence level of 95%
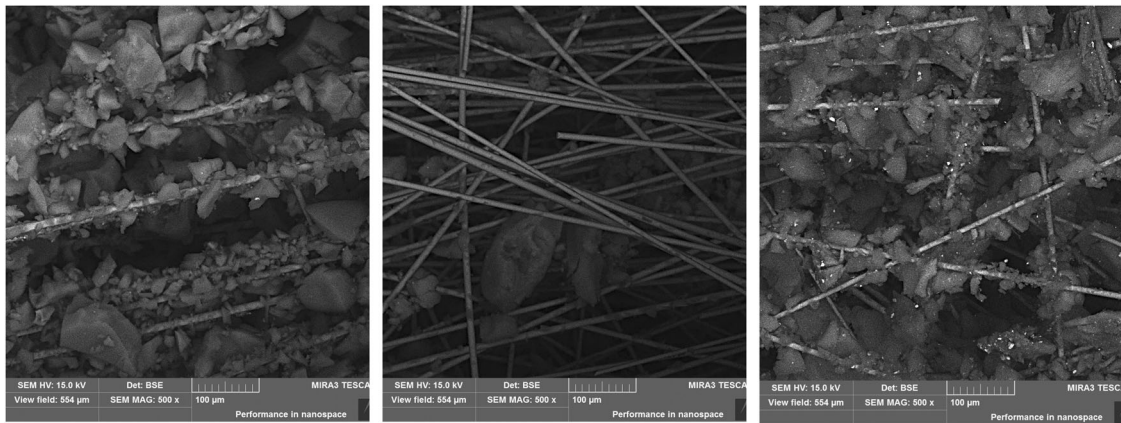
Fig. 2 Micrographs of sample A, B and the Pyrogel® aerogel blankets (from left to right) at low vacuum mode (7 Pa). SEM magnification ×500, BSE detector. Accelerating voltage 15 kV
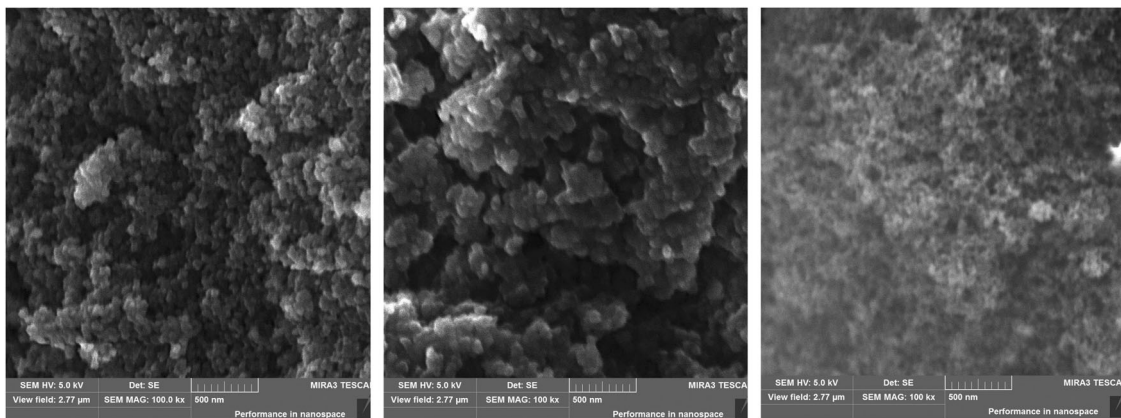

Fig. 3 Micrographs of sample A, B and Pyrogel® aerogel blankets (from left to right). SEM magnification ×100,000, SE detector. Accelerating voltage 5 kV

During the microscopic observation, the chemical composition of micro areas was also analysed by the EDS method. The limitations of this method should be, however, taken into consideration. First, the light elements: H, He, Li and Be cannot be identified. Second, the C analysis is often abandoned due to the contamination phenomenon. As a result of the interaction between the electron beam and carbon compounds from environment (usually deposited on the sample), the contribution of the carbon is considerably overestimated [27]. In our case, the carbon fraction was omitted because the specimen was vapourized with graphite prior to the chemical composition (high vacuum) measurements. Third, due to the type of preparation (no metallographic section), the results of chemical composition measurements in micro areas cannot be treated quantitatively. Taking into account the above-mentioned objections, the obtained analysis is therefore only qualitative. This analysis allows for a rough comparison of the chemical composition of samples. It is conventionally assumed that

there are three groups of elements: main—mass fraction exceeds 10%, secondary—from 1% to 10% and trace—<1% [27]. The concentration of the elements (wt%) is shown in Table 4. The results were divided into two parts: fibre—the fibre material of the blanket; granule—which corresponds with aerogel deposited on the fibre. The qualitative material analysis shows that both the fibres and the aerogels of all the samples have analogous elements. In the case of fibres, the main elements are always O, Si, Ca, and the secondary is Al. In the case of the granules, the main components are Si and O, to which Ca compounds and to a lesser extent Al compounds can be added. It can therefore be stated that all the materials are, from the chemical point of view, materials belonging to the same group of compounds. Differences in the presence of trace elements may result from the different raw materials used in the manufacturing process or deliberate use of additives. For example, as observed in Table 4, traces of titanium (sample B) could potentially come from TiO_2, which is a known

Table 4 Weight concentration of elements in granules and fibres of the A, B and Pyrogel® samples

Elements	Sample A		Sample B		Pyrogel®	
	Granule (%)	Fibre (%)	Granule (%)	Fibre (%)	Granule (%)	Fibre (%)
O	57.1	43.1	57.9	50.7	58.0	47.7
Si	40.8	37.5	36.6	25.2	37.4	26.2
Na	0.1	0.4	–	0.2	–	0.4
Mg	–	0.5	–	0.4	–	0.4
Al	0.6	5.4	1.3	7.6	1.7	7.8
S	0.1	–	–	–	–	–
K	–	0.2	–	–	–	–
Ca	1.3	12.9	3.4	14.7	2.4	16.9
F	–	–	–	0.8	–	0.6
Ti	–	–	0.4	0.4	–	–
Fe	–	–	–	0.5	–	–
Total		100		100		100

opacifier [28, 29]. Analogous concentrations of Fe in the Pyrogel® sample probably come from Fe_3O_4, another opacifier. Such mineral powder loading is especially important in decreasing the thermal conductivity value at high temperatures [30–35]. Although there are trace amounts of only these elements in the samples, it is difficult to be certain if they were deliberately added to the sample as radiation scattering agents, especially as the amounts of Ti and Fe did not correspond to the literature data [29, 36].

4.3 Maximum service temperature

The results of the maximum service temperature tests for sample A are presented in Figs. 4 and 5. Figure 4 shows the stability of the temperature value on the hot side of the sample and the temperature at half of the thickness of the sample during 72 h of the measurements. The temperatures of sample A were recorded at the expected maximum service temperature of 750 °C.

The change of the thickness during the heat treatment ($\Delta\varepsilon_d$) on sample A is also presented. The maximum value, $\Delta\varepsilon_d$, was 4.7%, and did not exceed 5%. So with such an assumption ($\leq$5%) the maximum service temperature could be established at 750 °C for sample A.

To ensure that the maximum service temperature of 750°C was the highest value of temperature of sample A, further tests were performed. Figure 5 shows the values of temperatures of sample A which were recorded at an expected maximum service temperature of 780 °C together with the change of the thickness during the heat treatment. The dimensional change of thickness, $\Delta\varepsilon_d$, was 5.2%. Due to exceeding the assumption, which was $\leq$5%, the maximum service temperature was established at 750 °C for sample A.

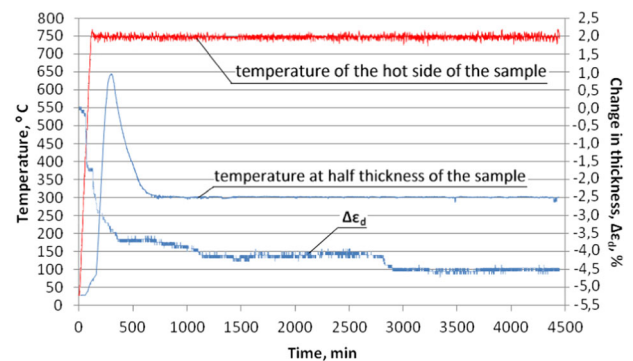The results of the maximum service temperature tests for sample B are shown in Figs. 6 and 7. Figure 6 shows

Fig. 4 Temperature (°C) dependence vs. time (min) and dimensional change of thickness, $\Delta\varepsilon_d$ (%), of sample A at the estimated/expected maximum service temperature of 750 °C
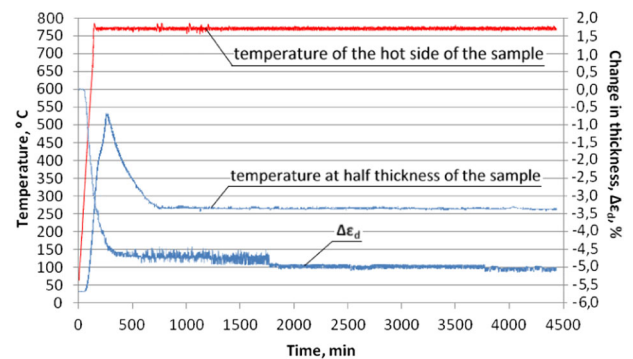

Fig. 5 Temperature (°C) dependence vs. time (min) and dimensional change of thickness, $\Delta\varepsilon_d$ (%), of sample A at the estimated/expected maximum service temperature of 780 °C

stability of the temperature value on the hot side of the sample and temperatures at half of the thickness of sample B during 72 h at the expected maximum service temperature of 600°C. The change of the thickness during the heat treatment ($\Delta\varepsilon_d$) on sample B is also presented. The dimensional change of thickness, $\Delta\varepsilon_d$, did not exceed 5%.
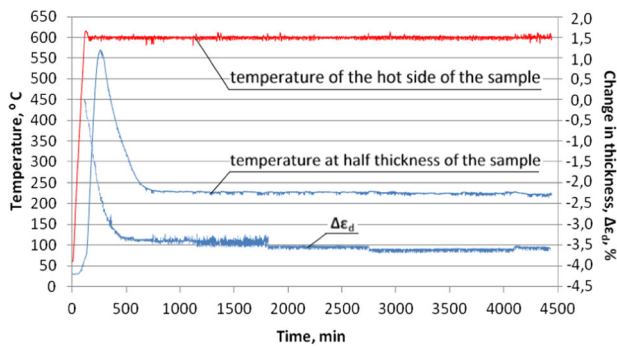
Fig. 6 Temperature (°C) dependence vs. time (min) and dimensional change of thickness, $\Delta\varepsilon_d$ (%), of sample B at the estimated/expected maximum service temperature of 600°C
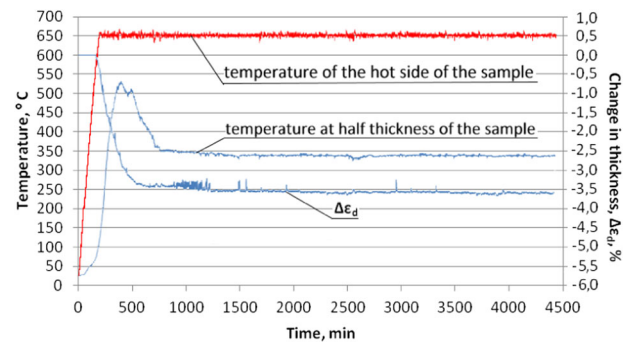

Fig. 8 Temperature (°C) dependence vs. time (min) and dimensional change of thickness, $\Delta\varepsilon_d$ (%), of the Pyrogel® sample at the estimated/expected maximum service temperature of 650°C
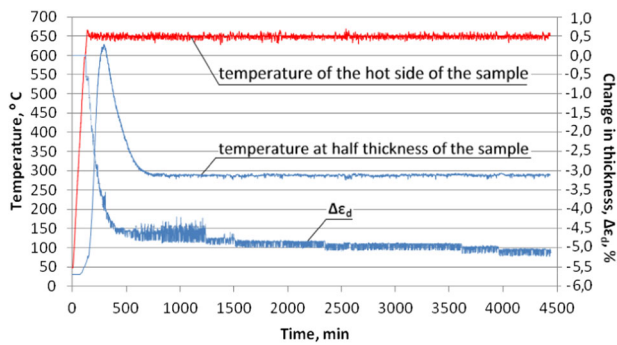

Fig. 7 Temperature (°C) dependence vs. time (min) and dimensional change of thickness, $\Delta\varepsilon_d$ [%], of sample B at the estimated/expected 650°C maximum service temperature

Assuming a change ≤5%, the maximum service temperature could be established at 600 °C for sample B.

To ensure that the established maximum service temperature at 600 °C was the highest value of temperature of sample B, further tests were performed. Figure 7 shows the values of temperatures of sample B which were recorded during the expected maximum service temperature of 650 °C together with the change of thickness during the heat treatment. The dimensional change of thickness, $\Delta\varepsilon_d$, was 5.2%. Due to exceeding the assumption, which was ≤5%, the maximum service temperature should not be established at 650 °C for sample B.

The results of the maximum service temperature tests for the Pyrogel® sample are shown in Fig. 8 showing the stability of the temperature value on the hot side of the sample and temperatures at half of the thickness of the Pyrogel® sample during 72 h of measurement. The temperatures of the Pyrogel® sample were recorded during the expected maximum service temperature of 650 °C. In Fig. 8 the change of the thickness during the heat treatment ($\Delta\varepsilon_d$) on the Pyrogel® sample is also presented. The dimensional change of thickness, $\Delta\varepsilon_d$, did not exceed 5%. So in such an assumption (≤5%), the maximum service temperature could be established at 650 °C for the Pyrogel® sample.

For all the investigated samples a rapid temperature increase at half of the thickness of the sample was observed during the heat treatment (Figs. 4–8). It started ca. 1 h after the beginning of heating side. The rate of temperature increase at half of the thickness of the sample was similar to the rate of sample heating, 5 °C/min. The maximum temperature at the half-thickness was usually reached after ca. 3–5 h of heating, depending on the maximum temperature value. Then, the temperature of half of the thickness of the sample started to drop until reaching ca. half of the maximum temperature value of the sample. A similar effect was observed with mineral wool products [34, 35, 37, 38] and the effect is called internal self-heating. Its source in mineral wool products is due to exothermic reactions occurring in the binder (phenol formaldehyde resin) [35]. The observed effects in aerogel samples may be explained by the low volume of the heat capacity, due to the high porosity of the materials, which do not absorb significant amount of heat and let the temperature rise (very low diffusivity of the materials), or by the reaction of organic compounds (e.g. from hydrophobization) at high temperature.

According to such an explanation, the higher temperature on hot plate induces higher temperature at half-thickness of the sample, as observed in Fig. 6 (a temperature of 600 °C in such condition induced a temperature at half-thickness of ca. 570 °C) and in Fig. 7 (a temperature of 650 °C in such condition induced temperature at half-thickness ca. 630 °C). Similar effect is noticed for sample A (Figs. 4 and 5). Comparing temperatures at half of the thickness of the samples, it is noticed that for higher temperature of the hot side (780 °C) the temperature at half of the thickness of the sample is lower (c.a.530 °C Fig. 5), than for lower temperature of the hot side (750 °C), where temperature at half-thickness of the sample is ca. 645 °C. Probably, the explanation can be correlated with the change in the thickness for sample A in Fig. 4. The smaller change in thickness of the
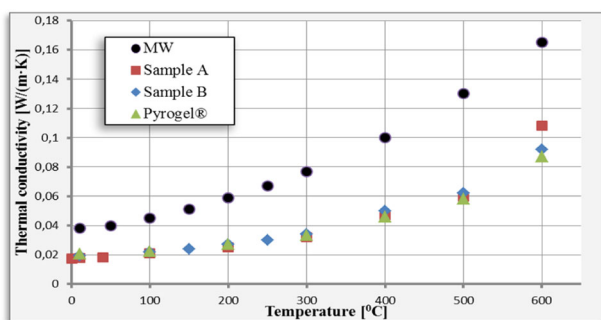
Fig. 9 Evolution of the thermal conductivity vs. temperature of samples A, B, Pyrogel® and mineral wool (stone)

sample leads to longer path for the heat transfer and higher temperature at half-thickness of the sample.

These observed effects in aerogels blankets will be a subject of further investigation.

4.4 Thermal conductivity test

The thermal conductivity of samples A, B and Pyrogel® are presented in Fig. 9 for a wide range of mean temperatures (from 10 to 600 °C). Additionally, together with the investigated aerogel samples, the data of mineral wool (stone wool) [39] were added to compare different, high temperature thermal insulation products available on the market.

The highest mean temperature was set at 600 °C due to the maximum service temperature of product B and the Pyrogel® product (see subsection Maximum service temperature under the Results section). During the tests in the range of temperatures from 400 to 600 °C the difference of plate temperatures (ΔT) were 100 K, meaning that the hot plate, together with a guarded heater, was set to 650 °C, and that the two cold plates were set to 550 °C. The higher temperature of the thermal conductivity test (650 °C) should not affect the Pyrogel® properties. For sample B, however, the higher temperature set on the hot plate together with the guarded heater was higher than the maximum service temperature measured for this product and could have slightly affected the thermal properties of sample B. But, finally, although the maximum service temperature measured for sample B was 600 °C, the thermal conductivity test was performed at a mean temperature of 600 °C (with $\Delta T = 100$ K) on account of the producer's declared specifications (the declared maximum service temperature was 650 °C; Table 1). Comparing the behaviours of the three blankets (Fig. 9), it is seems that there was no effect on the thermal properties of sample B.

The evolution of thermal conductivity vs. the temperatures of the samples A, B, Pyrogel® and mineral wool (stone) in the literature data are also not linear, because at

higher temperatures, the radiation increases its role in heat transfer as observed in Fig. 9.

For each temperatures, up to 550 °C, the values of the thermal conductivity of samples A, B and Pyrogel® are practically the same. However, at 600 °C the difference of the thermal properties between sample A and the Pyrogel® sample is ca. 20%. The answer as to why this happens is not the purpose of this article. However, the literature data [25, 26, 28–32] indicate a wide variety of solutions, and at least two careful considerations can be made. First, to decrease the influence of the radiation at higher temperatures, a mineral opacifier has been loaded to the aerogel products, as observed by the presence of titanium and iron compounds were noticed in sample B and the Pyrogel® (Table 4).

However, it should be mentioned that carbon black (which was not taken into consideration during the chemical analysis) or C compounds are also loaded into the aerogels as opacifiers to reduce the radiative heat transfer [40]. Therefore, in this area, our results are incomplete, and the possible role of impurities cannot be unambiguously identified. Second, the role of fibres is negligible in heat transfer. It is known that pure silica aerogels are transparent in the infrared wavelength range between 3 and 8 μm [41]. Thus, not only can fibres with appropriate parameters be used to strengthen the material but they can also be used as an opacifier. One of the important parameters is the thickness of the fibres loaded into aerogels. It was shown for amorphous SiO_2 glass fibres that the optimum thickness for the best thermal insulation performance is 4–8 μm [40]. It should be noted that the thickness of the fibres in sample A differs greatly from those of the samples B and Pyrogel® and only the diameter of sample A fibres is clearly outside its quoted thickness range. Thus, the latter discussed reason can be more unequivocal.

It seems that product B and Pyrogel® are more appropriate for higher temperature applications (pointing to Pyrogel®) than product A, which was characterized with better thermal properties at lower temperature applications (from 0 to 200 °C). Of course, the differences of the aerogel products' thermal properties are incomparably smaller (about half) of that of the mineral wool—the most popular product for industrial application.

5 Conclusions

The aim of this paper was to investigate the suitability of two new factory-made Chinese aerogel products available on the market for use in high temperature applications. The comparison of the dimensions stability, water vapour transmission, water absorption, maximum service temperature and thermal properties has been done with the product Pyrogel®.

The values obtained for the water vapour transmission and water absorption by immersion were correlated with the density of the samples. The values for all the investigated samples are at a level which allow to detect any of corrosiveness of the metal parts of installation.

An interesting behaviour was noticed during the maximum service temperature tests. For all the investigated samples, the internal self-heating for mineral wool products was observed. During the maximum service temperature measurements, when the temperature of one side of the sample increased up to the set temperature, a rapid rise (similar to the heating, but shifted in time) of the temperature at half of the thickness of the sample was observed for all aerogel samples. After ca. 3–5 h the temperature at half of the thickness of the sample started to drop. The observed effect in aerogel samples may be explained by the low volume heat capacity, due to the high porosity of the materials, and will be the subject of further investigation.

Among the aerogel samples investigated, the differences in thermal properties were observed. The differences of thermal properties can come from the different microstructure of samples—the number of granules on the fibres, and the aerogel's chemical composition. At higher temperatures the stronger influence of radiation was observed. It seems that opacifiers (TiO_2, Fe_3O_4) were loaded into the aerogel product B and Pyrogel® to reduce the influence of radiative heat transfer in the mineral wool. Additionally, the comparison of the thermal properties of the aerogel samples with that of the mineral wool showed a significant difference. These products are in particular dedicated for industrial, high temperature applications, and aerogels seem to be a solution for high-efficiency thermal industrial performance, especially at higher temperatures (energy savings compared to other insulating materials such as mineral wool).

Compliance with ethical standards

Conflict of interest The authors declare that they have no competing interests.

References

1. Greeley TR (1997) A review of expanded polystyrene (EPS) properties, performance and new applications. In: Graves RS, Zarr RR (eds) Insulation materials: testing and applications, vol 3. ASTM International, West Conshohocken, PA, USA

2. Koebel MM, Rigacci A, Achard P (2011) Aerogels for super-insulation: a synoptic view. In: Aegerter MA, Prassas M, Koebel MM (eds) Aerogels handbook—advances in sol-gel derived materials and technologies. Springer, New York, NY, Dordrecht, Heidelberg, London, pp 607–633

3. Papadopoulos AM, Giama E (2007) Environmental performance evaluation of thermal insulation materials and its impact on the building. Build Environ 42(5):2178–2187

4. Demharter A (1998) Polyurethane rigid foam, a proven thermal insulating material for applications between +130°C and −196°C. Cryogenics 38(1):113–117

5. Oertel G (1994) Polyurethane handbook, 2nd edn. Hanser, Munich

6. Ma Y, Wang J, Xu Y, Wang C, Chu F (2013) Preparation and characterization of phenolic foams with eco-friendly halogen-free flame retardant. J Therm Anal Calorim 114(3):1143–1151

7. Galbraith GH, Guo JS, McLean RC (2000) The effect of temperature on the moisture permeability of building materials. Build Res Inform 28(4):245–259

8. Fricke J, Schwab H, Heinemann U (2006) Vacuum insulation panels–exciting thermal properties and most challenging applications. Int J Thermophys 27: 1123. https://doi.org/10.1007/s10765-006-0106-6

9. Fricke J, Heinemann U, Ebert HP (2008) Vacuum insulation panels—from research to market. Vacuum 82:680–690

10. Baetens R, Jelle BP, Thue JV, Tenpierik MJ, Grynning S, Uvslokk S, Gustavsen A (2010) Vacuum insulation panels for building applications: a review and beyond. Energy Build 42:147–172

11. Baetens R, Jelle BP, Gustavsen A (2011) Aerogel insulation for building applications: a state-of-the-art review. Energy Build 43 (4):761–69

12. Koebel MM, Rigacci A, Achard P (2012) Aerogel-based thermal superinsulation: an overview. J Sol-Gel Sci Technol 63:315–339

13. Laskowski J, Milow B, Ratke L (2016) Aerogel–aerogel composites for normal temperature range thermal insulations. J Non-Cryst Solids 441:42–48

14. Miros A (2016) Thermal properties stability of organic thermal insulation materials for industrial insulation. Izolacje 3:78–81 (in Polish)

15. Gürtler A (2014) Minimising energy loss in industrial processes in the context of the European Energy Efficiency Directive. Conference "Heat not Lost", Cracow

16. Aspen Aerogels Inc. Northborough. http://www.aerogel.com. Accessed 30 Apri 2016

17. Cabot Corporation. http://www.cabotcorp.com. Accessed 30 Apri 2016

18. EN 822:2013. Thermal insulating products for building applications. Determination of length and width

19. EN 823:2013. Thermal insulating products for building applications. Determination of thickness

20. EN 1604:2013. Thermal insulating products for building applications. Determination of dimensional stability under specified temperature and humidity conditions

21. EN 12086:2013. Thermal insulating products for building applications. Determination of water vapour transmission properties

22. EN 12087:2013. Thermal insulating products for building applications. Determination of long term water absorption by immersion

23. EN 14706:2012. Thermal insulating products for building equipment and industrial installations. Determination of maximum service temperature

24. EN 12667:2001 Thermal performance of building materials and products. Determination of thermal resistance by means of

guarded hot plate and heat flow meter methods. Products of high and medium thermal resistance

25. Fomitchev DV, Trifu R, Gould G (2004) Fiber reinforced silica aerogel composites: thermal insulation for high-temperature applications. engineering, construction, and operations in challenging environments. https://doi.org/10.1061/40722(153)132

26. Kwon YG, Choi SY, Kang ES, Baek SS (2000) Ambient-dried silica aerogel doped with TiO_2 powder for thermal insulation. J Mater Sci 35:6075–6079

27. Goldstein J, Newbury D, Joy D, Lyman D, Echlin P, Lifshin E, Sawyer L, Michael J (2008) Scanning Electron Microscopy and X-ray Microanalysis, 3rd edn. Springer Science & Business Media, LLC, New York, NY

28. Wang J, Kuhn J, Lu X (1995) Monolithic silica aerogel insulation doped with TiO_2 powder and ceramic fibers. J Non-Cryst Solids 186:269–300

29. Wang X-D, Sun D, Duan Y-Y, Hu Z-J (2013) Radiative characteristics of opacifier-loaded silica aerogel composites. J Non-Cryst Solids 375:31–39

30. Lu X, Caps R, Fricke J (1995) Correlation between structure and thermal conductivity aerogels of organic. J Non-Cryst Solids 188:226–234

31. Lee D, Stevens PC, Zeng SQ, Hunt AJ (1995) Thermal characterization of carbon-opacified silica aerogels. J Non-Cryst Solids 186:285–290

32. Rombouts M, Froyen L, Gusarov AV, Bentefour EH, Glorieux C (2005) Light extinction in metallic powder beds: correlation with powder structure. J Appl Phys 98:013533

33. Rettelbach T, Sauberlich J, Korder S, Fricke J (2005) Thermal conductivity of in-opacified silica aerogel powders between 10K and 275K. J Phys D 28(1995):581–587

34. Gray BF (2016) Spontaneous combustion and self-heating. In: Hurley MJ, Gottuk DT, Hall Jr JR, Harada K, Kuligowski ED, Puchovsky M, Torero JL, Watts Jr JM, Wieczorek CJ (eds) SFPE handbook of fire protection engineering, Springer, New York, NY, USA, p 604–632

35. Spokoinyi FE, Eidukyavichus KK (1988) Mechanism of spontaneous ignition during storage of mineral wool objects. Combust Explos Shock Waves 24(6):649–651

36. Yu H-T, Liu D, Duan Y-Y, Wang X-D (2014) Theoretical model of radiative transfer in opacified aerogel based on realistic microstructures. Int J Heat Mass Transfer 70:478–485

37. Walker IK, Harrison WJ (1960) The self-heating of wet wool. N Z J Agric Res 3(6):861–895

38. EN 14303:2009 Thermal insulation products for building equipment and industrial installations. Factory made mineral wool (MW) products. Specification

39. Miros A (2012) Flat products for thermal insulation of buildings and industrial installations. Izolacje 9:42–45 (in Polish)

40. Zhao J-J, Duan Y-Y, Wang X-D, Wang B-X (2012) An analytical model for combined radiative and conductive heat transfer in fiber-loaded silica aerogels. J Non-Cryst Solids 358:1303–1312

41. Fricke J, Tillotson T (1997) Aerogels: production, characterization, and applications. Thin Solid Films 297(1997):212–223